AIMS Environmental Science

AIMS Environmental Science, 10 (3): 398–423.
DOI: 10.3934/environsci.2023023
Received: 19 November 2022
Revised: 03 March 2023
Accepted: 22 March 2023
Published: 04 May 2023

http://www.aimspress.com/journal/environmental

Research article

Spatiotemporal analysis of drought occurrence in the Ouergha catchment, Morocco

Kaoutar MOUNIR[1,2,*], Isabelle LA JEUNESSE[2,4], Haykel SELLAMI[3] and Abdessalam ELKHANCHOUFI[1]

[1] University Sidi Mohamed Ben Abdallah of Fez, CED ST LGE2D, Fez, Morocco
[2] University of Tours, UMR CNRS 7324 Citeres, 33 allée Ferdinand de Lesseps, 37204 Tours cedex 3, France
[3] Centre for Water Research and Technology, EcoPark BorjCedria, Soliman, Tunisia
[4] UMR 7300 ESPACE, Université Côte d'Azur, Mediterranean Institute of Environmental Risk and Sustainable Development, Nice Meridia Technopole, 9, Rue Julien Lauprêtre, 06200 Nice, France

* **Correspondence:** Email: kaoutar.mounir@univ-tours.fr; Tel: +33-247361487.

Abstract: Although the spatiotemporal characterization of droughts is a key step in the design and implementation of practical measures to mitigate their impacts, it is hampered by the lack of hydro-climatic data with sufficient spatial density and duration. This study aimed to assess the trends and spatial patterns of drought occurrence in the Ouergha catchment in northern Morocco, which has been identified as a hot spot for climate change and variability. The study combined data from various sources, including the North Atlantic Oscillation Index (NAOi); Western Mediterranean Oscillation Index (WeMOi); a meteorological index (SPI), calculated using precipitation data; a hydrological index (SDI), calculated using precipitation data; and satellite images to calculate the Normalized Difference Vegetation Index (NDVI) and Normalized Difference Moisture Index (NDMI) from 1984/85 to 2016/17. The results showed that the adopted statistical analyses were effective in detecting the linearity and trend of drought in the Ouergha catchment scale. The correlations between various indices were moderate to strong between NAOi and SPI, WeMoi and SPI, as well as SPI and SDI, while the Mann-Kendall tests indicate an increasing trend of drought intensity in the catchment. During dry events, vegetation cover and moisture were maintained due to the presence of dam reserves. Overall, the study provides empirical evidence that confirms the severe drought conditions experienced in the Ouergha catchment. The unique set of data adds to the growing body of knowledge about drought in the region and underscores the urgency of preserving dam resources for

sustainable use during future droughts.

Keywords: drought; SPI; SDI; vegetation indices; Ouergha catchment

1. Introduction

Droughts are among the most important natural hazards affecting large populations and have significant consequences for the economy, the environment and societal development. Drought frequency and impacts are expected to be exacerbated by changing climate and land use conditions in the Mediterranean, particularly in areas already exposed to weather-related disasters [1]. Drought is one of the most complex weather-related disasters and can persist for months and years [2], negatively impacting the environment and socio-economic development, and it increases conflicts among political and economic actors [3]. From a climatic perspective, drought is defined as a precipitation shortage that persists over an extended period and is characterized by its intensity, duration and extent. Thus, the spatiotemporal characterization of drought is a key step in the design and implementation of adaptive measures [4].

By its climatic characteristics and geographical position, Morocco has experienced many severe droughts in the last years which could potentially experience up to five consecutive years of drought without interruption. Due to the recurrent drought events and the trend of decreasing precipitation, water resources are expected to worsen in the future [5–7]. The Intergovernmental Panel on Climate Change projections indicate a strong warming trend for Morocco. Since 1970, there has been an observed temperature increase of about 3 to 7°C are projected for Morocco by 2100, particularly for the summer months (from June to August). Annual precipitation is expected to decrease by 10 to 30% during the wet season (from October to April), and a 10 to 40% decline during the dry season (from May to September) [8,9]. In the upcoming years, Morocco will be more exposed to drought, unless action is taken [9,10] . Thus, this variability has negative impacts on agriculture, which is mainly rain-fed and very vulnerable to climatic variations [9,10]. Water scarcity has imposed the need for resource management to adapt the policy of dams to store the inputs of wet years in favor of dry years, and also to transfer water to deficit regions to ensure water availability and food security at the country level.

Several studies have used various approaches to understand drought impacts and predict its occurrence. One approach has been to analyze the interactions between ocean-atmospheric oscillation indices and meteorological and hydrological drought indices in critical areas worldwide [11–15]. Another approach is to model drought, which can help identify risk areas, predict the timing and severity of droughts and support decision-making for drought mitigation and management despite the complex interactions between atmospheric and continental processes.

In addition, several researchers have sought to show how the atmospheric circulation patterns lead to precipitation shortages in different regions worldwide by using statistical approaches. For example, Luppichini [16] investigated the correlation between the North Atlantic Oscillation Index (NAOi) and precipitation trends in Tuscany, Italy; Lopez-Bustins and Lemus-Canovas [17] showed the spatiotemporal relationship between the Western Mediterranean Oscillation (WeMOi) influence and precipitation irregularity in Catalonia. For Morocco, Zamrane [18] revealed significant correlation between hydrological variability and climatic fluctuations materialized by different

climatic indices such as the NAOi, the Southern Oscillation Index (SOI) and the WeMOi. Furthermore, Driouech et al. [10] evaluated the relationships of climate extremes in Morocco linked to NAOi using drought indices and showed that the NAO effect on Moroccan precipitation extends to the October–February period. In addition, El Niño–Southern oscillation (ENSO) does not affect Morocco; regarding teleconnections other than NAO, Mediterranean oscillation (MO) plays an important role in Morocco's humid and semi-arid areas. Still, more research is required for the interactions between these teleconnections and the effects of local scale topographical conditions [9].

Drought monitoring can be based on a single variable to compute meteorological and hydrological drought by using, for example, the percent of normal precipitation index [19], the standardized precipitation index (SPI) [20], the standardized water-level index [21] and the streamflow drought index (SDI) [22] . Remote sensing indices, such as the normalized difference vegetation index (NDVI), have been widely applied to characterize spatiotemporal drought indices at different timescales [23]. The 3-, 6- and 12-month scales are typically used to represent short-, medium- and long-term droughts, respectively. In addition, atmospheric circulation-drought calculation methods are subject to uncertainty [24].

Most of the few studies on climate trends in Morocco have been conducted either at the national scale or catchment level. Several studies have been conducted in Morocco to understand and address the impact of droughts on agriculture and water resources. As a national scale example, Ezzine et al. [25] developed a new drought index, i.e., the Standardized Water Index (SWI), based on the Normalized Difference Water Index (NDWI), and compared its performance with other indices. The study found a strong correlation between SWI and cereal production; Verner et al. [9] assessed the effects of droughts on the agricultural sector and evaluated the government's efforts to address them, using indices such as ENSO, NAO and MO to analyze the impact of teleconnections. The study highlighted the importance of effective drought management. Regarding examples of specific case studies in Morocco, Boudad et al. [26] analyzed the characteristics of meteorological and hydrological droughts in the Inaouen basin of northern Morocco over different timescales, using the SPI and SDI to assess the droughts. The results showed that the frequency of drought episodes varies with the timescale, and that there is a strong positive correlation between the SPI and SDI at the 12-month scale. Moreover, Hadri et al. [27] analyzed the relationship between vegetation activity and drought severity in the western Haouz plain in Morocco over a 10-year period, using satellite images and indices such as the SPI and SWI. The study found a clear relationship between vegetation activity and drought severity.

The previous research offers valuable insights into the drought trends across Morocco, but there is a lack of studies that specifically focus on the impact of atmospheric circulation patterns on drought in the Ouergha catchment. This catchment plays an important role in agricultural production and the mobilization of its conventional water resources. By combining atmospheric oscillations and meteorological (SPI) and hydrological (SDI) drought indices, the assessment of the vulnerability of the Ouergha catchment to drought can be improved.

The aim of this study was to assess the trends and spatial patterns of drought occurrence in the Ouergha catchment in Morocco using the SPI and SDI, multisource data from local hydroclimatic records, remote sensing and the large-scale NAOi and WeMOi. Therefore, this paper evaluates trends in precipitation, flow rate and extreme indices at the Ouergha catchment scale using the SPI and SDI derived from 10 meteorological stations and eight hydrometric stations covering all of the main climate zones of the catchment. Then, we examined the relationship between drought indices and the

NAOi and WeMoi indices to assess the usefulness of drought indices (SPI and SDI). In addition to assessing detailed trends at the catchment scale, we also conducted trend analysis at the stations scale. Finally, we present spatial distribution maps of drought indices, derived from temporal SPI and SDI values, as well as vegetation moisture and density states during dry events. These maps aim to demonstrate the spatial distribution of drought and its effects on land use in the Ouergha catchment.

2. Materials and methods

2.1. Study area

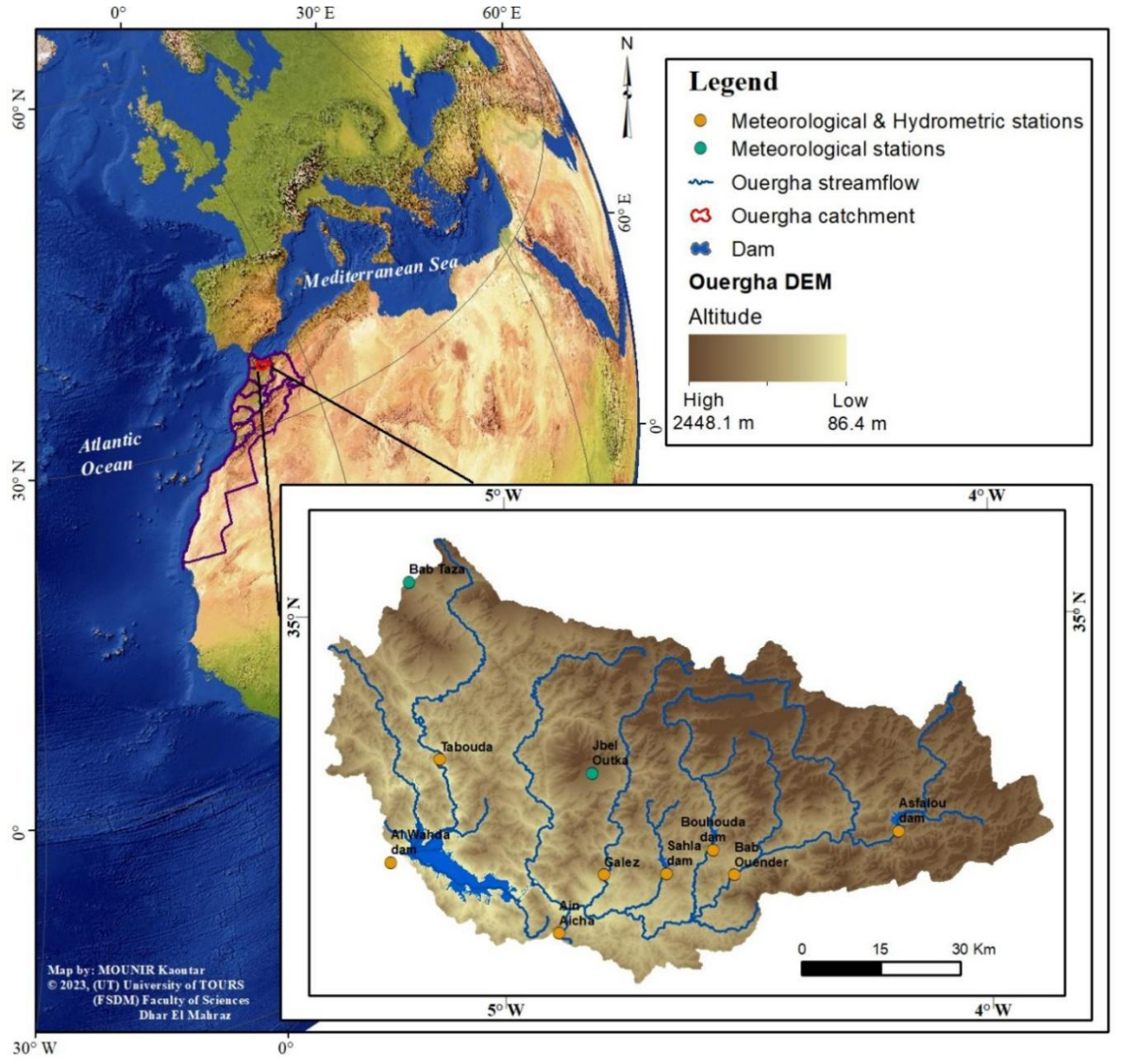

Figure 1. Geographic location of the Ouergha catchment.

The Ouergha catchment is the principal tributary of the Sebou catchment, located between 34°20'N and 35°10'N and 3°55'W and 5°20'W. The catchment covers approximately 6,190 km^2 and supplies "Al Wahda", the largest dam in Morocco, with an annual storage capacity of 3800 Mm^3 [28] (Figure 1). The catchment has deeply dug shale beds, with tormented relief and deep gorges. The largest part of the catchment is marked by a sharp relief with domed summits located on the eastern

side, while the northern boundary of the catchment, representing the summit of the Rif chain, consists almost entirely of a grit bar more resistant than shale and includes the most important summits in the basin that are east–west-oriented sandstones. The course of the Ouergha river contains poorly drained, hilly relief with many signs of erosion [29]. The southern part of the Ouergha catchment intersects with the extremely complex Pre-Rifain system and the limestone massifs of the southern border. The Ouergha Valley is dominated by alluvial terraces with shallow soils occupied by many crops [30]. The catchment has a Mediterranean climate with a dry season that varies according to altitude, annual average precipitation ranging from 800 mm to more than 1000 mm at high altitudes, and a rainy season that starts in November and ends in April. During summer, air temperatures can exceed 40 °C [29], giving important weight to evapotranspiration and its influence on the water flow balance [28]. The Northern ridge line of the catchment, which is marked by mountains, experiences westerly winds that bring rain and affects 78% of the area. However, the downstream part of the basin forms an isolated catchment that benefits less from the precipitations input of the western and southern areas [30]. The Mediterranean climate of the area is typically subject to stormy precipitation, the intensity of which can influence the amount of water flowing under torrential conditions. The Ouergha river is formed by the intersection of Asfalou river to the east and the highest part of Ouergha river to the north and passes through the Bab Ouender hydrometric station [30]. The streamflow of the Ouergha catchment is characterized by high intra-annual variability, with the lowest and highest flows from June to September and December to February, respectively [31]. The rivers in the Ouergha catchment, except for the Sahla river, are fed by melting snow on the mountains, while the predominance of clay and the presence of disaggregated layers of marl and shale increase the impermeability of the catchment, thus explaining the lack of groundwater in the Ouergha catchment [28].

2.2. Datasets

2.2.1. Local hydro-climate data

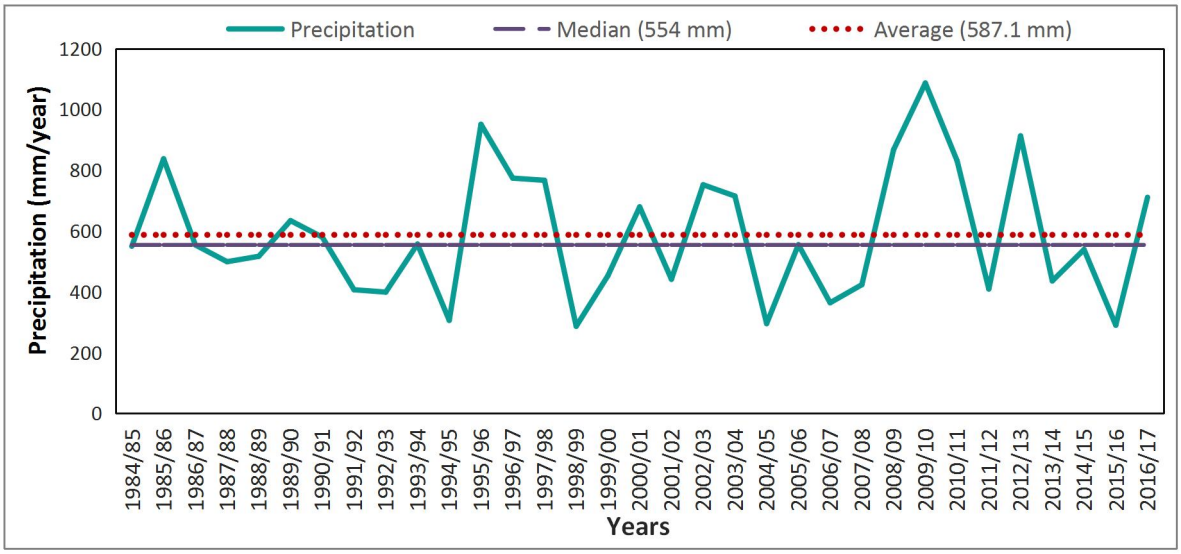

Figure 2. Annual average precipitations in the Ouergha catchment for 33 years.

Data on precipitations and flow rate were obtained from the SHBA (Sebou Hydrological Basin

Agency), which collects data from meteorological and hydrometric stations spread across the basin. Unfortunately, not all stations were selected for this study due to some being abandoned or having recently been set up. Only stations with a consistent and sufficient record length were selected for analysis, resulting in the inclusion of 10 meteorological stations and 8 hydrometric stations, all covering a 33-year period from October 1984/85 to September 2016/17.

The average annual precipitations for 10 meteorological stations for 33 years was 587.1 mm (median of 554 mm) (Figure 2). The precipitation ranged between 286 mm (in 1998/99) and 1086 mm in 2009/10. The graph shows an unbalanced average precipitation during the 33 years, with amounts below average from 1986/87–1988/89, 1990/91–1994/95, 1998/99–1999/00, 2001/02, 2004/05–2007/08, and 2013/14–2016/17. The latter periods alternated with two- to three-year humid periods with precipitations exceeding 600 mm.

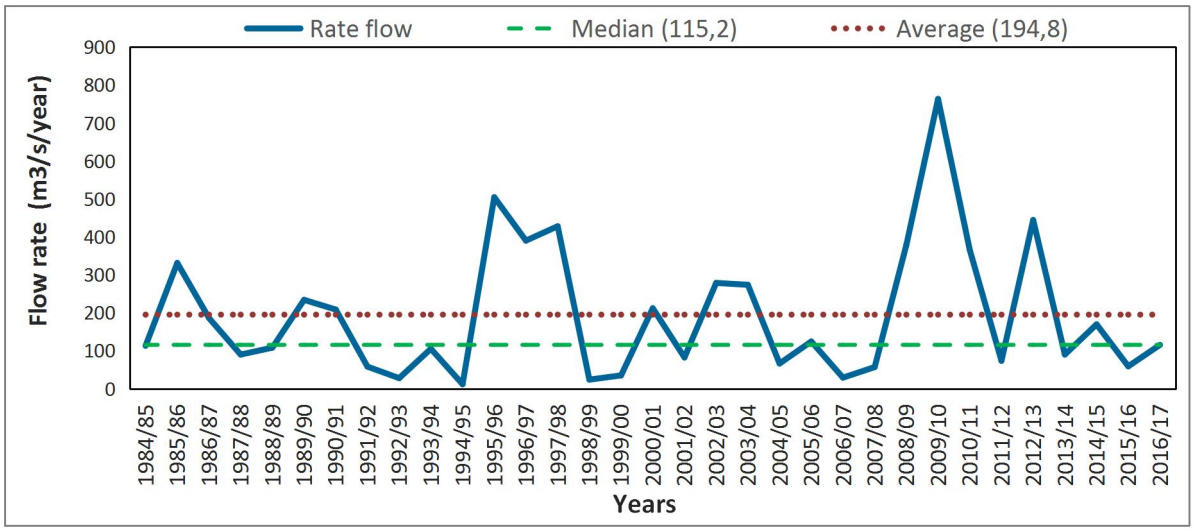

Figure 3. Annual average rate flow curve in the Ouergha catchment for 33 years.

The average annual rate flow for 8 hydrometric stations for 33 years was 194.8 m^3/s (median of 115.2 m^3/s) (Figure 3). The rate flow ranges between 11.5 m3/s in 1994/95 and 763.3 m^3/s in 2009/10. The graph shows an unbalanced average precipitations during the 33 years, with amounts below average from 1984, 1986/87–1988/89, 1991/91–1994/95, 1998/99–1999/00, 2001/02, 2004/05–2007/08, 2011/12 and 2013/14–2016/17. The latter periods alternated with two- to three-year humid periods with rate flow ranges between 208.1 in 1990/91 and 763 m^3/s in 2009/10.

2.2.2. Large-scale NAO and WeMoi

Historical records of monthly and annual NAOi were obtained from the US National Oceanic and Administration website. The NAOi is the difference in the surface pressure anomalies between various northern and southern locations that tracks seasonal movements of the Icelandic low and Azores high.

The recorded WeMOi data for the study period were acquired from the website of the Climatology Group of Barcelona University (http://www.ub.edu/gc/wemo/). WeMOi is the atmospheric connection between a point to the southwest of San Fernando and the Po Valley of Padua [32] and is calculated from the surface pressure data of the Global Forecast System (GFS), a

model developed by the National Centers for Environmental Prediction (NCEP), an agency within the National Oceanic and Atmospheric Administration (NOAA) of the United States. The WeMOi data is updated with model outputs at 0h and 12h, and it covers up to 144 hours. WeMOi is used during the autumn months as a predictive tool for torrential rains. Moreover, NAOi and WeMOi cover the period from 1984/85–2016/17.

2.2.3. Remote sensing data

Satellite-based vegetation observations provide a complementary method for monitoring and analyzing the spatial extent and variability of the effect of drought on vegetation conditions. The most commonly used method to monitor vegetation is through long-term, global-scale datasets of vegetation cover based on passive satellite observations since the 1970s. These datasets are highly valued by researchers and policymakers because they offer consistent and long-term data on vegetation cover over large areas [33]. Nevertheless, in this particular study, we analyzed the impact of drought on vegetation conditions using data bands from the Landsat TM5 and Landsat OLI 8 sensors (Table 1, Table 2, Table 3). The satellite images used in the study were typically from the spring season when vegetation is denser, to investigate the vegetation's growth potential in response to water and soil moisture levels. This choice of season was particularly important as any drought-induced impact on vegetation growth would be reflected in the vegetation index, which reflects the chlorophyll content and vitality of the growing vegetation.

Table 1. Landsat sensor characteristics (http://landsat.gsfc.nasa.gov/).

Characterization	Landsat 5		Landsat 8	
Sensors	TM		OLI	
Launch	01-March-84		11-February-13	
End of mission	05-June-13		To date	
Orbit Altitude	705 Km		705 Km	
Orbit	Quasi-polar heliosynchronous		Quasi-polar heliosynchronous	
Field of view	185 Km		185 Km	
Average resolution	General: 30 m; Thermal infrared: 120 m		General: 30 m; Panchromatic: 15 m; Thermal infrared: 100 m	
Coverage	16 days		16 days	
Limitations	Limited spectral resolution and the fact that it stopped operating in 2013, making its data less relevant for recent analyses		Limited spectral resolution compared to hyperspectral sensors and the fact that cloud cover can hinder observations in certain areas	
Used images date	Left image	Right image	Left image	Right image
	16/02/1993	25/02/1993	22/05/2016	15/05/2016
	13/05/1995	19/03/1995		
	21/03/1999	30/03/1999		
	08/05/2005	17/05/2005		
	19/03/2007	29/04/2007		
	22/05/2016	15/05/2016		
Source	https://earthexplorer.usgs.gov/			

Table 2. Spectral bands of Landsat 5 TM sensor (http://landsat.gsfc.nasa.gov/).

Bands	Spectral bands	Wavelength	Spatial resolution
1	Blue	0.45–0.52 µm	30 m
2	Green	0.52–0.60 µm	30 m
3	Red	0.63–0.69 µm	30 m
4	Near-infrared	0.76–0.90 µm	30 m
5	Near-Infrared	1.55–1.75 µm	30 m
6	Infrared-thermal	2.08–2.35 µm	120 m
7	Mid-infrared	2.08–2.35 µm	30 m

Table 3. Spectral bands of the Landsat 8 OLI sensor (http://landsat.gsfc.nasa.gov/).

Bands	Spectral bands	Wavelength	Spatial resolution
1	Coastal Aerosol	0.43–0.45 µm	30 m
2	Blue	0.45–0.51 µm	30 m
3	Green	0.53–0.59 µm	30 m
4	Red	0.63–0.67 µm	30 m
5	Near infrared	0.85–0.87 µm	30 m
6	Medium Infrared 1	1.56–1.65 µm	30 m
7	Medium Infrared 2	2.10–2.29 µm	30 m
8	Panchromatic	0.50–0.67 µm	15m
9	Cirrus	1.36–1.38 µm	30 m
10	TIRS 1	10.60–11.19 µm	100 m
11	TIRS 2	11.50–12.51 µm	100 m

2.3. Methods

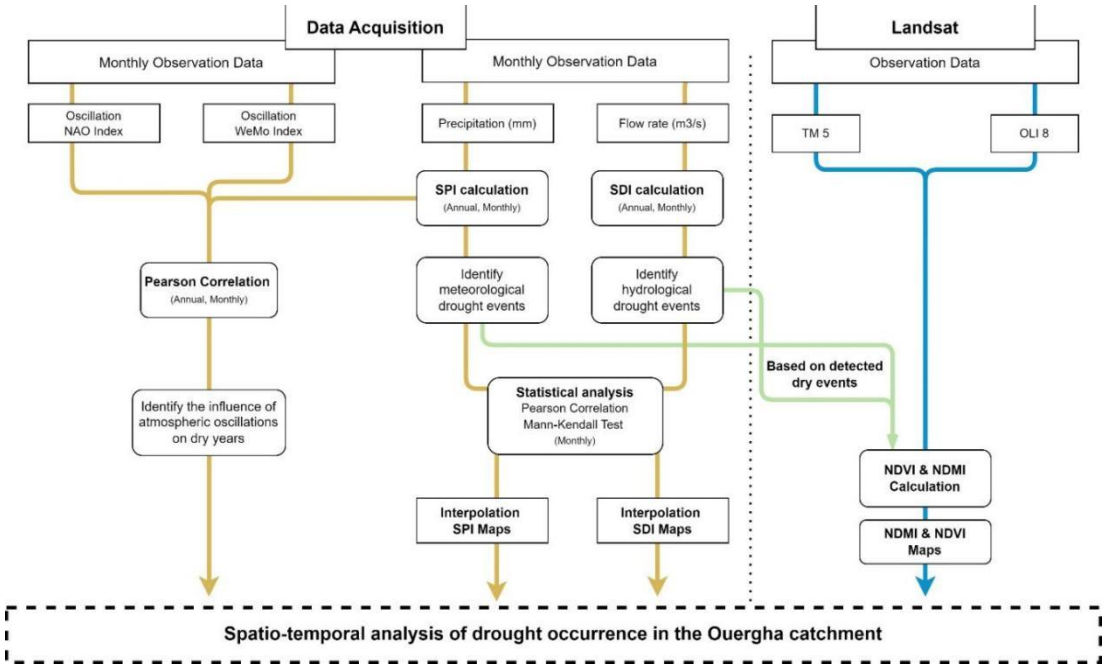

Figure 4. General framework flowchart of the adopted methodology.

As shown in the general framework flowchart (Figure 4), multi-step formulation was carried out to assess trends and spatial patterns of drought occurrence in the Ouergha catchment.

2.3.1. Drought indices

The Standardized precipitation index (SPI) was developed by McKee et al. [20] as a method for defining and monitoring drought occurrences. It is a simple index [22,26] that relies solely on precipitation data and enables the evaluation of both wet and dry periods. Different time scales can be used to calculate the SPI, reflecting the impact of drought on different types of water resources. The computation of SPI for a specific site is based on a long-term precipitation record, spanning over 30 years, and is fitted to a probability distribution, such as the Gamma distribution. The SPI is computed using the following equation:

$$SPI_{i,k} = \frac{X_{i,k} - \overline{X_k}}{S_k} \qquad \text{i=1,2, 3…, k=1,2,3,4} \tag{1}$$

where: Xi,k is the cumulative precipitation amount for the k-reference period of the hydrological year (i) or month (k). N indicates the number of hydrological years. Sk is the standard deviation of the cumulative precipitation of the reference period k.

The Streamflow drought index (SDI), developed by Nalbantis and Tsakiris [22], is used to assess hydrological drought. The SDI is based on monthly observed flow rate and offers the advantage of monitoring hydrological drought and water supply over short, medium, and long terms. The index is calculated based on cumulative rate flow for each reference period in a given hydrological year, using the following equation:

$$SDI_{i,k} = \frac{V_{i,k} - \overline{V_k}}{S_k} \qquad \text{i=1,2, 3…, N; k=1,2,3,4} \tag{2}$$

where: Vi,k is the cumulative flow amount for the k-reference period of the hydrological year (i). N indicates the number of hydrological years. Sk is the standard deviation of the cumulative streamflow volumes of the reference period k.

Table 4. Classification of the SPI and SDI values (modified).

Index values	Classification
SPI (SDI) > 2	Extremely wet
1.5 < SPI (SDI) < 1.99	Very wet
1 < SPI (SDI) < 1.49	Moderately wet
-0.99 < SPI (SDI) < 0.99	Mildly wet
-1 < SPI (SDI) < 0	Mildly dry
-1.5 < SPI (SDI) < -1	Moderately dry
-2 < SPI (SDI) < -1.5	Severely dry
SPI (SDI) < -2	Extremely dry

According to Nalbantis et al. [22], a dry event occurs when the index continuously reaches an intensity of -1.0 or higher; each drought event is marked by a notable duration and intensity. Table 4 displays the state of the meteorological and hydrological drought classifications [22].

2.3.2. Vegetation indices

The NDVI [23] and NDMI [34] are important indices used in remote sensing analysis. The measurements of near-infrared (NIR), red (R), and short-wave infrared (SWIR1) were taken from the bands of Landsat satellite images, which were chosen due to their widespread availability and high spatial and temporal resolution, making them suitable for remote sensing analysis (Table 1, Table 2, Table 3). These bands were processed with both radiometric correction and atmospheric correction to correct variations in the sensor response and ensure that the image data accurately reflects the reflectance properties of the Earth's surface and remove or correct the effects of atmospheric absorption, scattering, and other factors that can impact the measured radiance values. The correction process was carried out using ENVI 5.3 software, and the atmospheric correction was specifically conducted using the FLAASH (Fast Line-of-sight Atmospheric Analysis of Spectral Hypercubes) module.

NDVI is based on the contrasting characteristics of two bands in a multispectral raster dataset, represented by the absorption of chlorophyll pigments in the R band and the high reflectivity of plant materials in the NIR band (Table 2, Table 3). The NDVI is constructed by combining the R and NIR bands and expressed using the following equation:

$$NDVI = \frac{NIR - R}{NIR + R} \tag{3}$$

NDMI uses two bands to monitor drought and display the canopy humidity level and fuel level in fire-prone areas. The index is computed using NIR and short-wave infrared reflectance (SWIR) (Table 2, Table 3) and is expressed using the following equation:

$$NDMI = \frac{(NIR - SWIR1)}{(NIR + SWIR1)} \tag{4}$$

The calculation of NDVI and NDMI was conducted using ArcMap, which is the main component of the ArcGIS suite. The NDVI and NDMI values range from -1 to 1. Generally, values between 0 and 1 indicate higher levels of vegetation cover (NDVI) and moisture (NDMI), while values between 0 and -1 are indicative of water.

2.3.3. Trend analysis

This study analyzed the correlation between the NAOi, WeMOi, SPI, and SDI during the study period at different timescales. Pearson correlation was used to analyze the annual and monthly variability of meteorological and hydrological droughts. Accordingly, the absolute value of the correlation coefficient (r values) was computed using Eq 5, where r ranges between -1 and +1, and the highest r value (positive or negative) represents a higher correlation. The test was calculated at a confidence level of $P < 5\%$.

$$r(x_J y) = \frac{b.s_x}{s_y} = \frac{\left(\frac{1}{n}\sum_{i=1}^{n} x_i \gamma_i\right) - \overline{x} \cdot \overline{\gamma}}{\sqrt{\left(\frac{1}{n}\sum_{i=1}^{n} x_i^2\right) - (\overline{x})^2} * \sqrt{\left(\frac{1}{n}\sum_{i=1}^{n} \gamma_i^2\right) - (\overline{\gamma})^2}} \quad (5)$$

The non-parametric Mann–Kendall [35] test was used to detect monotonic trends in monthly, seasonal, and annual time series, does not require a normal distribution, and compares the relative magnitudes of the sample data rather than the data values themselves [36] . The Mann–Kendall statistic and the trend test for a data series are computed according to Eqs 6 and 7, respectively:

$$S = \sum_{i=1}^{N-1} \sum_{j=i+1}^{N-1} Sign(yj - yi) \quad (6)$$

$$Sign(yj - yi) = \begin{cases} 1 & if \quad yj - yi > 0 \\ 0 & if \quad yj - yi = 0 \\ -1 & if \quad yj - yi < 0 \end{cases} \quad (7)$$

where S is the statistic of the Mann–Kendall test; yi and yj are the annual values in years i and j (j > i), respectively; N is the length of the data series, and Sign is the sign (+ or -) of (yi– yj).

$$Z = \begin{cases} \dfrac{S-1}{[\sqrt{Var(S)}]^{\frac{1}{2}}} & if\ S > 0 \\ \qquad if\ S = 0 \\ \dfrac{S+1}{[\sqrt{Var(S)}]^{\frac{1}{2}}} & if\ S < 0 \end{cases} \quad (8)$$

The standard test statistic (Z) demonstrates an increasing trend with positive values, and the negative values show a decreasing trend in the time series. If |Z| > Z1 − α/2, the hypothesis of no trend is rejected, where |Z| and α indicate the absolute value of the Mann–Kendall coefficient and the statistical significance level, respectively.

Based on the Z-score, the trend in the data can be classified as significant, weak, or non-existent. For a significance level of 0.05, if the Z-score is greater than or equal to 1.96, this indicates a significant trend in the data, with a positive Z-score signifying an upward trend and a negative Z-score indicating a downward trend. If the Z-score falls between 1.0 and 1.96, this indicates a weak trend in the data. Finally, if the Z-score is less than 1.0, this suggests a lack of trend in the data [37].

3. Results

3.1. Drought trend analysis

The Ouergha catchment experienced varying annual precipitation and flow patterns with some years characterized by heavy precipitations and others by low precipitations (Figure 5). The precipitations exceedance probability (Figure 5, left) was generated for 10 meteorological stations

(Figure 1). The stations of Jbel Outka (at an altitude of 1090 m) and Bab Taza (at an altitude of 880m) recorded higher levels of precipitation with annual averages exceeding 1000 mm and 1500 mm respectively. Conversely, the precipitation recorded at Sahla dam station (at an altitude of 321 m) was much lower with an average of 20 mm. The remaining seven stations recorded average annual precipitation levels between 542 mm and 807 mm.

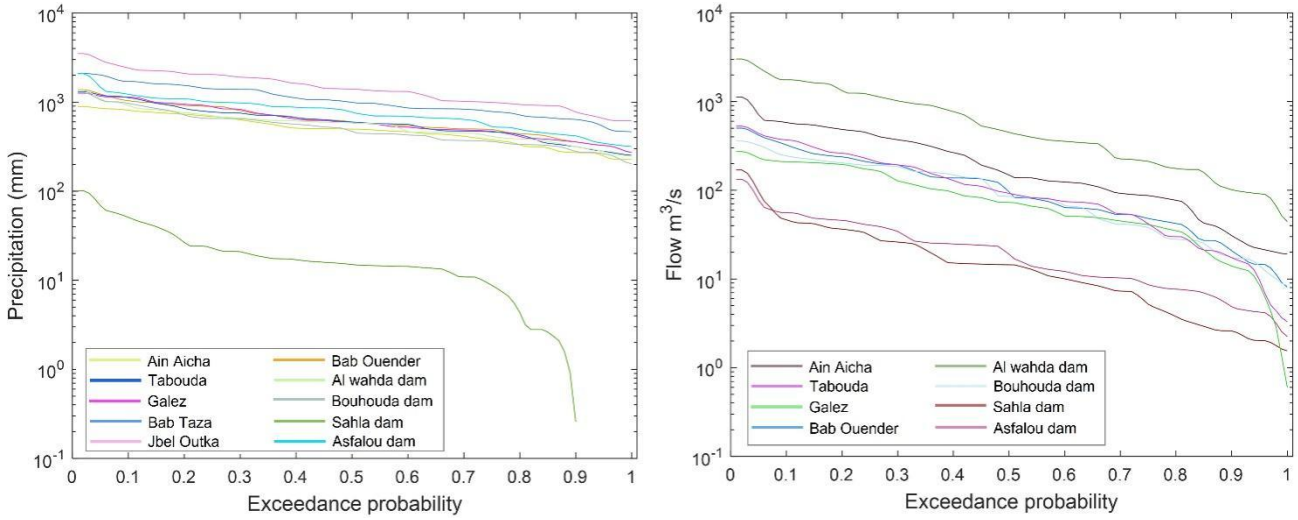

Figure 5. Exceedance probability curves for selected precipitations (left) and flow rates (right) stations in the Ouergha catchment.

The flow exceedance probability (Figure 5, right) constructed using data from 8 hydrometric stations (Figure 1). Each station recorded its highest and lowest flow rates at different times, resulting in a variation of flow rates across the stations. The Al Wahda dam station, located in the downstream region, has the highest flow rate at 755 m^3/s. On the other hand, the lowest flow rates were detected at the Asfalou and Sahla Dam stations with 26 m^3/s and 22 m^3/s, respectively. The remaining six stations had an average annual flow rate that falls between 96 m^3/s and 254 m^3/s.

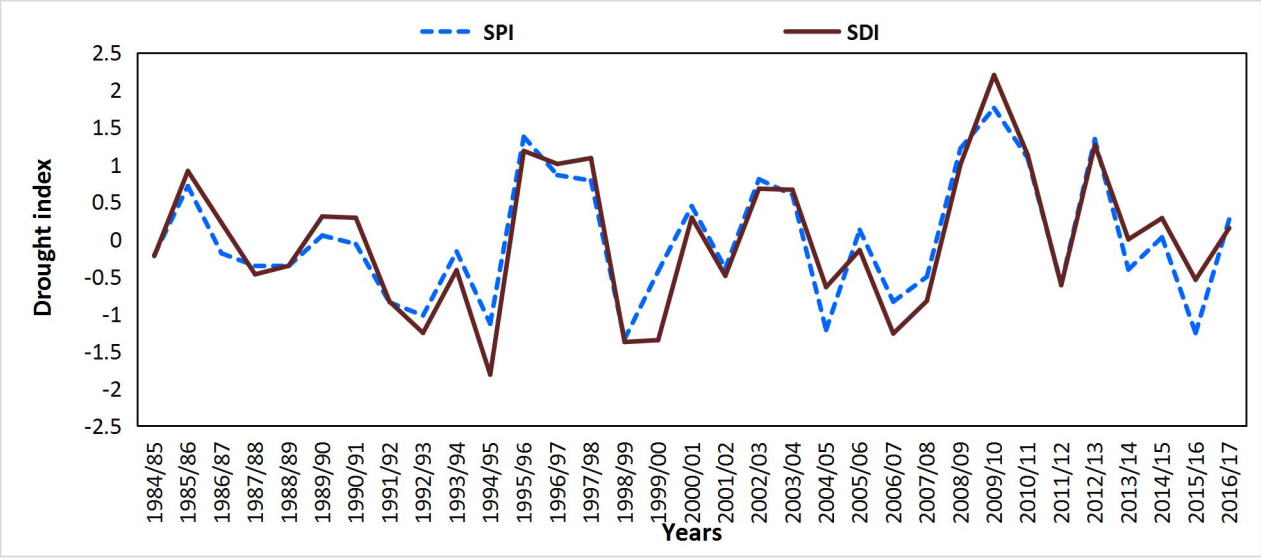

Figure 6. Temporal SPI and SDI values in the Ouergha catchment from 1984/85–2016/17.

Meteorological and hydrological parameters varied considerably within the study area. To explain the water shortage during the study period, Figure 6 shows the graphical representation of the calculated SPI and SDI. The two indices show concordant decreases and increases, indicating a close relationship between the two series. This can suggest that dry and humid events are succeeding one another, with changes in one index closely corresponding to similar changes in the other. The computed SDI and SPI are dry events when the index is equal to or below 1.0; a humid event is denoted by index values reaching or exceeding 1.0 (Table 2). The SDI reflects precipitations irregularities during the 33-year period in the form of moderate to severe dry events (-1.5 < SPI (SDI) < -1) in 1992/93, 1994/95, 1998/99, 2004/05, 2006/07, and 2015/16. The most severe hydrological stress during the 33-year period was observed in 1994/95, with a recorded average annual precipitation of 368.4 mm.

3.2. Pearson correlation

To detect the presence of linearity and to visualize the relationship between the atmospheric circulation indices (NAOi & WeMOi) and the meteorological drought index (SPI) in the Ouergha catchment, we applied the Pearson correlation coefficient on annual and monthly time-scale correlations at a significance level of 5%. In addition, the correlation coefficients ranged between -1 and +1 and measured the strength of association between two variables. A large correlation is observed for coefficient values between ± 0.5 and ± 1. A moderate correlation is represented by values lie between ± 0.3 and ± 0.5; and a small correlation occurs for value between + 0.3 and 0.1 is small, and if smaller that 0.1 is trivial [38,39].

The atmospheric oscillation index data used were adjusted on a hydrological year time scale to fit the SPI and SDI time scale patterns. For the annual time scale, the SPI has large negative relationships with the NAOi and WeMOi of -0.62, and -0.69, respectively. These large negative relationships show the connection between the NAOi and WeMOi and SPI but do not indicate if either index exerts a major influence. Therefore, a monthly correlation must be tested (Figure 7). Monthly correlations were favored to seasonal for more accurate results, since the atmospheric oscillations indices have a larger intraseasonal variability.

Overall, the monthly correlation between NAOi and SPI indicates a large negative linearity from November to March (Figure 7a). The low correlation between SPI and NAOi only from December to March may be due to the fact that the NAOi index is strongly correlated with winter climate patterns in the region but may not have as strong an influence on precipitation patterns during other seasons. Other factors, such as the North African monsoon or local convective activity, may play a larger role in determining precipitation patterns during other times of the year. Additionally, the NAOi index may exhibit less variability during other seasons, making it less strongly correlated with precipitation.

Thus, the correlation between WeMOi and SPI (Figure 7b) has a higher to moderate negative linearity for all months except May and August, when the correlation is low. This results may be due to the fact that the WeMoi index is not the only factor affecting precipitation during this time period. Other factors, such as local land use and topography, may also play a significant role in determining precipitation patterns during this period. In addition, the WeMoi index itself may exhibit less variability during these months, making it less strongly correlated with precipitation.

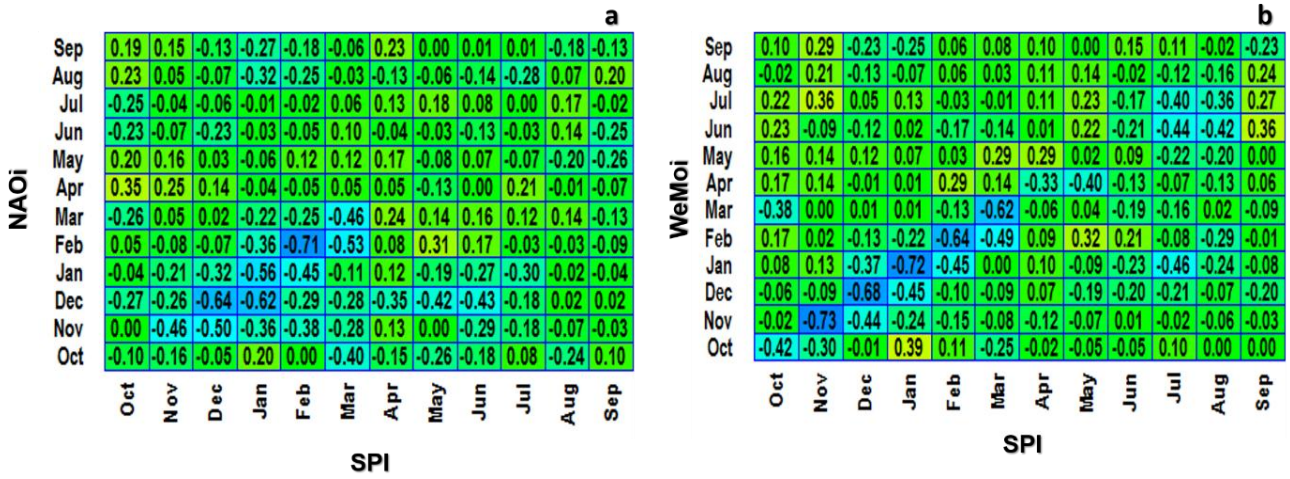

Figure 7. Correlogram of Pearson correlation coefficients between SPI and the atmospheric oscillation indices at a monthly scale from 1985–2017 at a level of significance alpha = 0.05. Large correlation: values between ± 0.50 and ± 1; moderate correlation: values between ± 0.3 and ± 0.5; small correlation: values between ± 0.3 and ± 0.1; smaller that 0.1 is trivial.

The SPI and SDI were calculated based on the average of the calculated indices for each meteorological and hydrometric station. The correlation between the indices displayed a large positive link for almost every month with a positive linearity (| r | > 0.60), except for July and August (Figure 8). Therefore, meteorological drought directly impacts the flow rate. The strong correlation is due to the dependency of the flow on precipitation, which can also be explained by the impermeability and very limited percolation of the catchment surface where stormwater runoff is predominant.

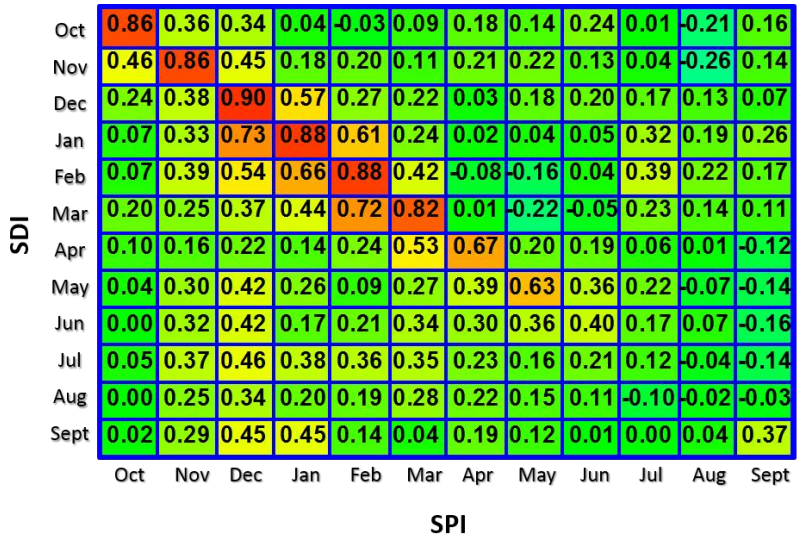

Figure 8. Correlogram of Pearson correlation coefficients between SPI and SDI at a monthly scale from 1985–2017 at a level of significance alpha = 0.05. Large correlation: values between ± 0.50 and ± 1; moderate correlation: values between ± 0.3 and ± 0.5; small correlation: values between ± 0.3 and ± 0.1; smaller that 0.1 is trivial.

3.2.1. Mann–Kendall test

The results of the Mann-Kendall test, represented as Z-scores, for the SPI across 10 meteorological stations and SDI for 8 hydrometric stations. The table 5 demonstrates that there are diverse trends across the various stations and months. Notably, some stations indicate significant trends, either positive or negative, while others exhibit no trend or only weak trends. It is crucial to consider the significant trends in the stations that could provide valuable insights into the increase or decrease of drought conditions within the SPI and SDI. However, weak trends are also considered helpful in providing valuable information about drought tendency.

Table 5. SPI trend of 10 meteorological stations in the Ouergha catchment at different time scales, for a significance level of 0.05. The colors in the table indicate: Blue: Z-scores greater than or equal to 1.96 indicate a significant trend in the data. Green: Z-scores between 1.0 and 1.96 indicate a weak trend. Grey: values less than 1.0 suggest a lack of trend. +: positive value; -: negative value.

Date	Ain Aicha	Bab Ouender	Galez	Tabouda	Bab Taza	Jbel Outka	Al Wahda dam	Asfalou dam	Bouhouda dam	Sahla dam
October	+	-	+	+	+	+	-	-	-	+
November	+	-	+	-	+	-	-	-	-	+
December	-	-	+	+	+	-	-	-	+	+
January	-	+	+	-	+	-	-	-	+	+
February	-	+	+	+	+	-	-	-	+	+
March	+	-	+	+	-	-	-	-	+	+
April	-	+	-	-	-	+	+	-	+	+
May	-	+	-	+	-	-	-	-	+	+
June	+	-	-	+	-	-	-	-	+	-
July	+	+	+	+	-	+	+	-	+	+
August	+	+	+	+	+	+	+	-	-	-
September	+	-	+	+	+	-	+	-	-	-

Table 5 reveals negative significant trends during the autumn negative significant trends were observed, while positive significant trends were noted in the autumn season, specifically in September and October at the Galez station, from September to November at the Bab Taza station, and in November at the Sahla Dam station. Weak negative trends were identified in the Bab Ouender station in September, in the Bouhouda dam station from September to October, and in the Asfalou dam station in October. Meanwhile, a positive weak trend was observed in the Tabouda station. During the winter, a significant positive trend was found in December at the Bab Ouender station and from December to February at the Sahla Dam station. Weak negative trends were observed in the Ain Aicha station in February and in Jbel Outka in January, as well as in the Asfalou dam from January to February. Positive weak trends were observed in January and February in Galez and in Bab Taza in January. During the spring, the Bab Ouender station showed a negative trend in March, whereas Bouhouda dam station had positive trends in March and May, and the Sahla dam station had a

positive trend in May. Additionally, weak positive trends were noted in Galez in March, Jbel Outka and Bouhouda dam in April, and Sahla dam station from March to April, while negative weak trends were observed in Galez in April, Jbel Outka and Al Wahda dam stations in March, and Asfalou dam in April and May. During the summer, the Jbel Outka station indicated negative trends in June and positive trends in August, while Bouhouda Dam station had a negative trend in August. Weak trends included a positive trend in Tabouda in August and in Bouhouda in June, while negative trends were observed in Bab Ouender in June, in Bab Taza from June to July, in Asfalou dam station in June and July, and in Sahla dam station in August.

Table 6. SDI trend of 8 Hydrometric stations in the Ouergha catchment at different time scales, for a significance level of 0.05. The colors in the table indicate: Blue: Z-scores greater than or equal to 1.96 indicate a significant trend in the data. Green: Z-scores between 1.0 and 1.96 indicate a weak trend. Grey: values less than 1.0 suggest a lack of trend. +: positive value; -: negative value.

Date	Ain Aicha	Bab Ouender	Galez	Tabouda	Al dam	Wahda	Asfalou dam	Bouhouda dam	Sahla dam
October	-	-	+	+	+		-	+	+
November	+	-	+	-	+		-	+	+
December	+	-	+	-	+		+	+	+
January	-	-	+	+	+		+	+	+
February	+	-	+	+	-		+	+	-
March	+	-	+	+	+		+	+	+
April	-	-	+	-	+		+	+	+
May	-	+	+	-	-		+	+	+
June	-	-	-	-	-		+	+	-
July	+	-	-	+	-		-	+	-
August	+	-	-	+	-		-	+	-
September	+	-	-	+	-		-	+	-

Table 6 indicates a single significant positive trend within the Tabouda station in August, while the other results demonstrate either weak trends or no trends. During the autumn, positive trends were detected in the Bouhouda dam and Tabouda stations in September and the Tabouda station in October. In the winter, negative weak trends were observed in the Bab Ouender station in February, while positive weak trends were noted in the Bouhouda dam station in December and January, the Al Wahda dam, Asfalou dam, and Sahla dam stations in January. During the spring, negative weak trends were found in the Bab ouender station during March and April, whereas the Galez station in March, the Tabouda station in May, and the Asfalou dam station in April showed positive weak trends. In the summer, negative weak trends were seen in the Ain Aicha station in June, the Bab ouender station in August, the Galez station in July, and the Tabouda station in June. Conversely, a positive weak trend was observed in the Bouhouda dam station in June and July.

3.3. Spatial drought detection

The correlation between the atmospheric oscillation indices and drought indices showed the solid atmospheric circulation effects on precipitation distribution in the Ouergha catchment, which is also related to the availability of water resources in rivers and dams. Furthermore, the SPI and SDI calculations provided more detailed results on drought occurrence in 1992/93, 1994/95, 1998/99, 2004/05, 2006/07, and 2015/16 (Figure 4). To further analyze drought event occurrence and water stress in the Ouergha catchment, the spatial patterns based on the SPI, SDI, NDVI, and NDMI are displayed in classes for severity levels greater than mild. Landsat images were used to visualize and quantify the effect of drought by computing the NDVI, which displays the vegetation evolution and the intensity of moisture using the NDMI.

Figure 9 shows the occurrence of drought in 1993. The highest drought level was 23% in the southern part of the catchment. To quantify the intensity of the drought in different parts of the catchment, we used the SDI, which measures the severity of hydrological drought. Our analysis showed that the SDI values were highest (approximately 49%) in the southwest and eastern parts of the catchment. This severe drought had a significant impact on the vegetation cover in the catchment, particularly in the eastern and southern parts, where it was low. This can be attributed to the fact that drought reduces soil moisture and limits plant growth. Furthermore, the spatial distribution of vegetation occupancy and moisture level in the Ouergha catchment showed that 88.31% of the catchment had a moisture level of 43%. These indices provide additional evidence of the impact of drought on vegetation cover in the catchment.

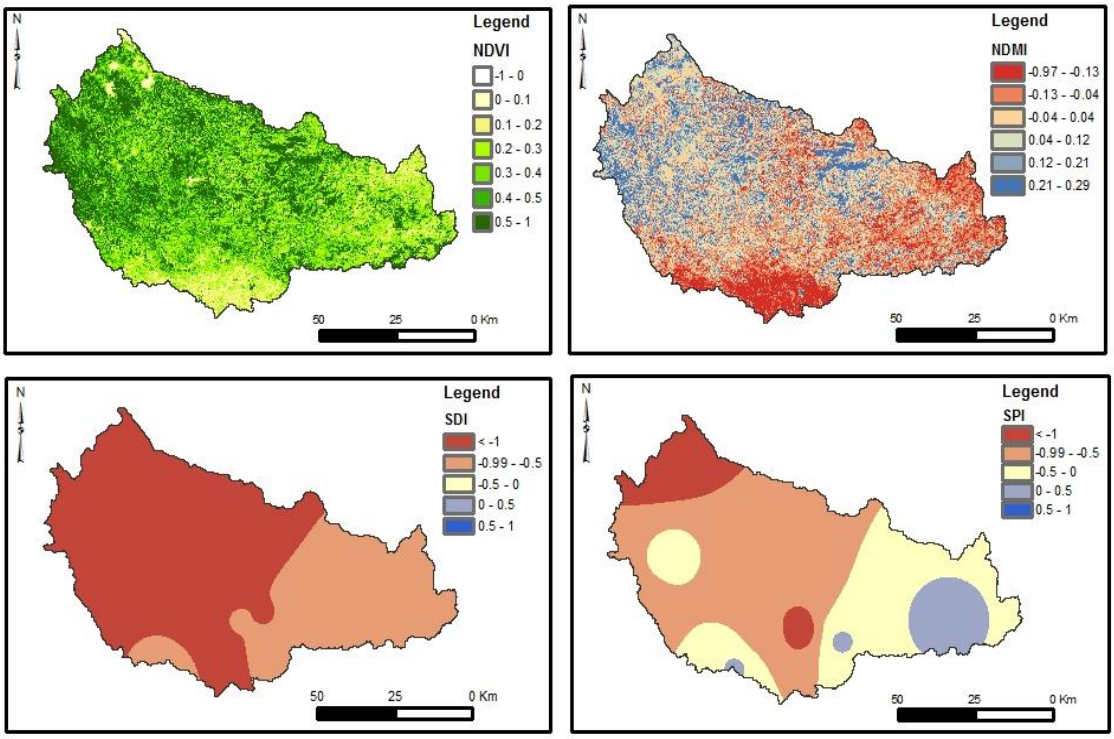

Figure 9. Spatial distribution maps of environmental variables and drought indices in the Ouergha catchment in 1993.

The commissioning of the Sahla dam, the first dam in the Ouergha Catchment, in 1994 coincided with the first extreme dry event that in 1994/95 (Figure 10). The occurrence of mild to moderate drought according to SPI values was observed in the eastern part of the catchment, representing approximately 55% of the total catchment area. SDI values indicated that a severe water deficit affected nearly all the catchment; and the percentages of the catchment experiencing moderate and severe drought were approximately 85% and 6%, respectively. Therefore, the vegetation was densest and wettest in the northern part of the catchment, which is a mountainous area. The southern part of the catchment had poor vegetation cover and experienced severe drought in 1995 as shown in NDVI map in Figure 10; spatial indices for the catchment showed vegetation and moisture levels of 88.81% and 39%, respectively.

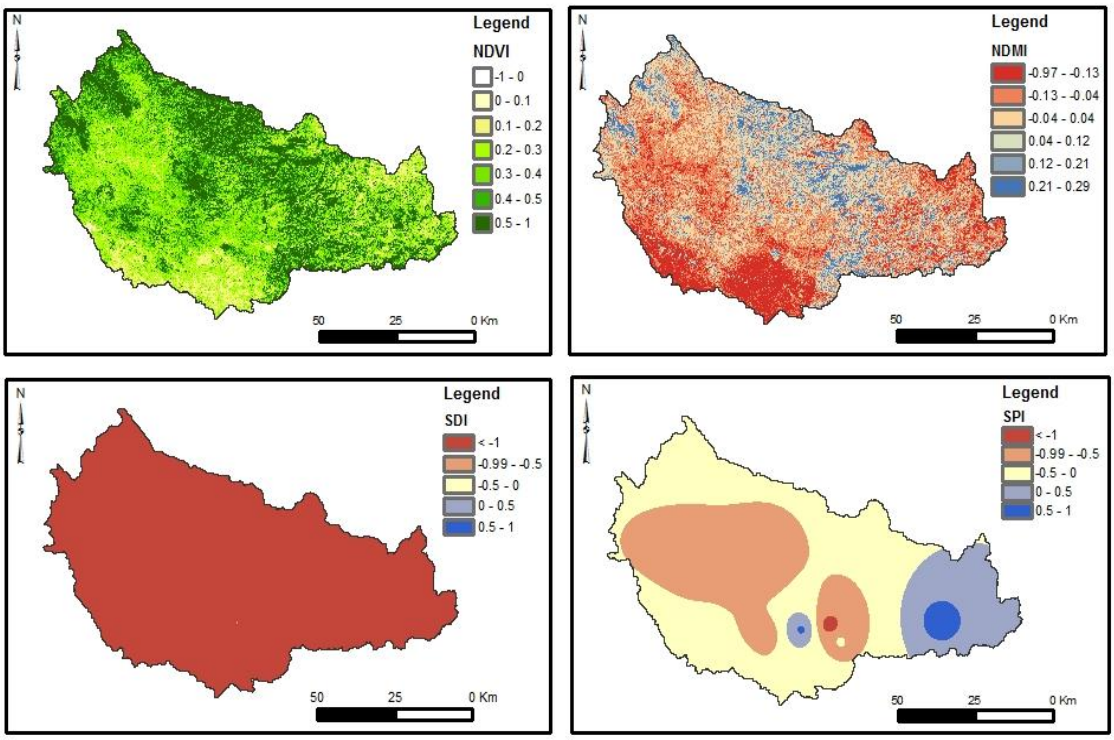

Figure 10. Spatial distribution maps of environmental variables and drought indices in the Ouergha catchment in 1995.

The Al Wahda (the second largest dam in Morocco), Bouhouda, and Asfalou dams were launched in 1996, 1998, and 1999, respectively. The dams were constructed to help provide siltation protection and continuous access to drinking water, to help promote irrigation in adjacent agricultural lands, and to cope with future drought periods. However, the dams did not help in 1999 (Figure 11), when the most severe meteorological drought in the history of the Ouergha Catchment impacted the hydrology and vegetation of the entire catchment. Vegetation cover fell 61.24%, and the level of moisture decreased to 20.52%.

Figure 12 shows that the meteorological drought was mild/moderate to severe in approximately 94% and 4% of the catchment, respectively. The SDI values in the catchment indicated mild dry events in the entire catchment, except the eastern part, which experienced severe drought. Nonetheless, the vegetation increased in 2005; and the NDMI showed moisture level of 46%. The densest vegetation was in irrigated areas surrounded by dams.

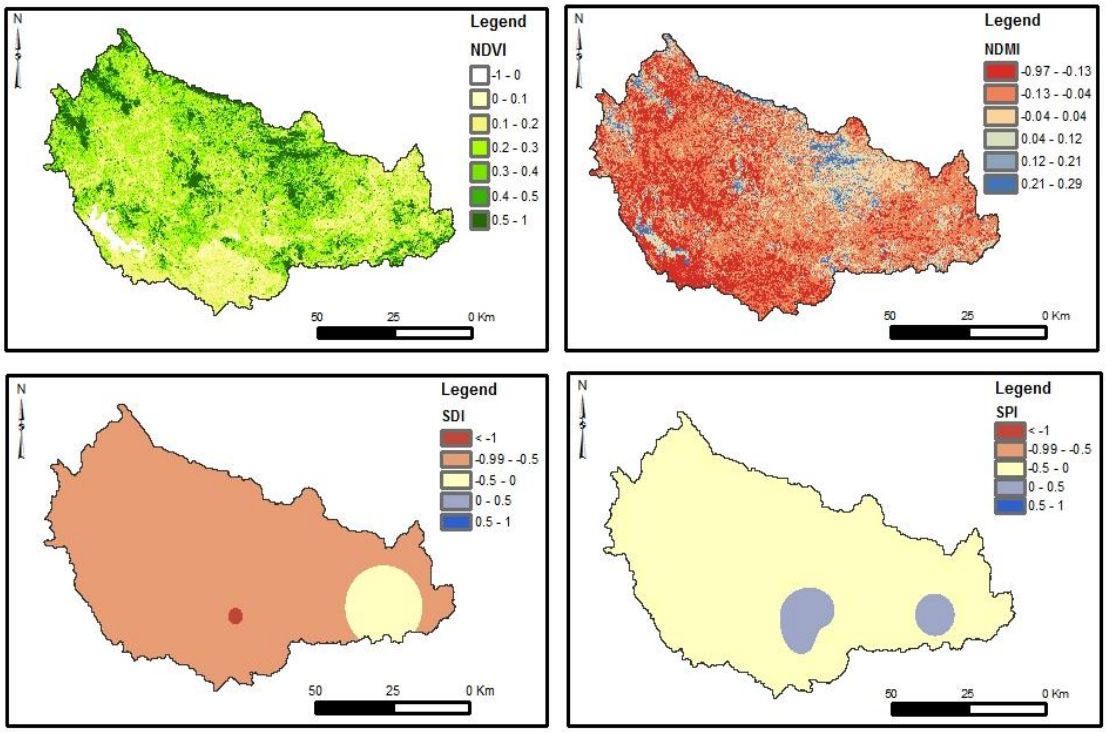

Figure 11. Spatial distribution maps of environmental variables and drought indices in the Ouergha catchment in 1999.

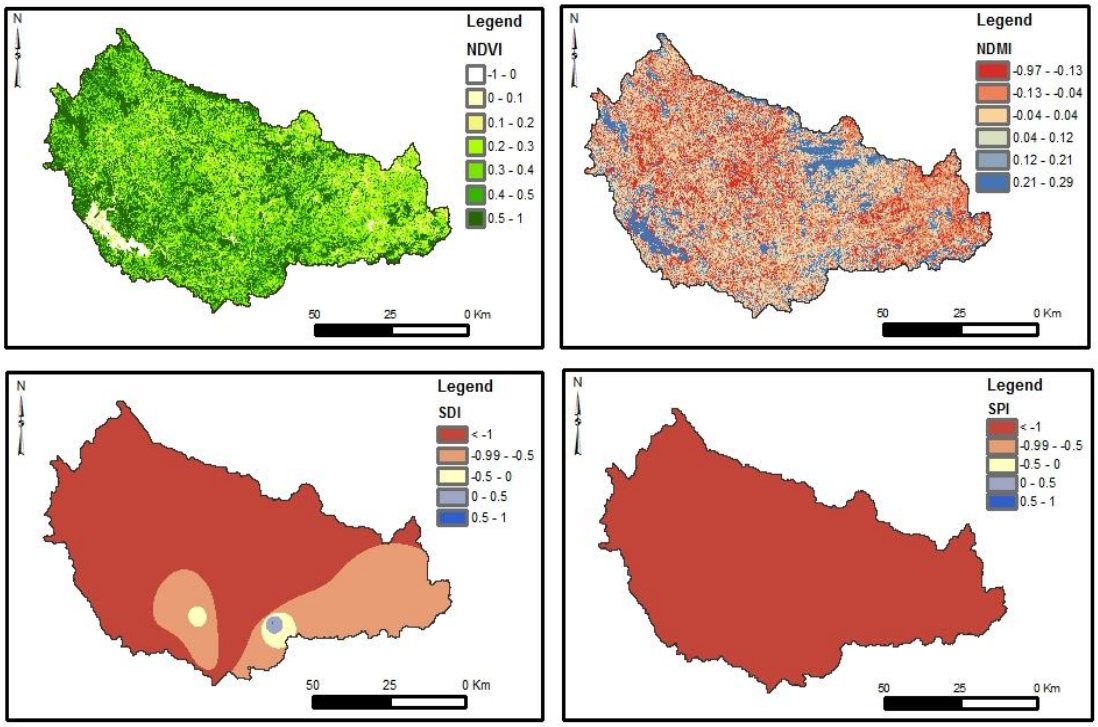

Figure 12. Spatial distribution maps of environmental variables and drought indices in the Ouergha catchment in 2005.

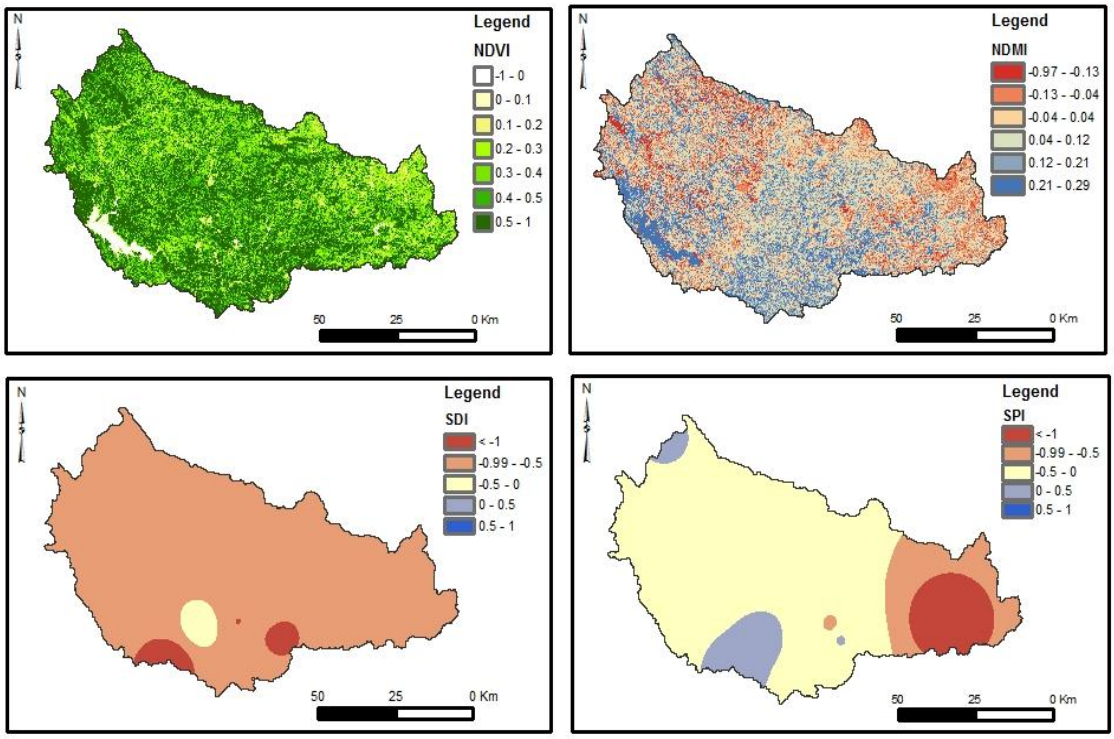

Figure 13. Spatial distribution maps of environmental variables and drought indices in the Ouergha catchment in 2007.

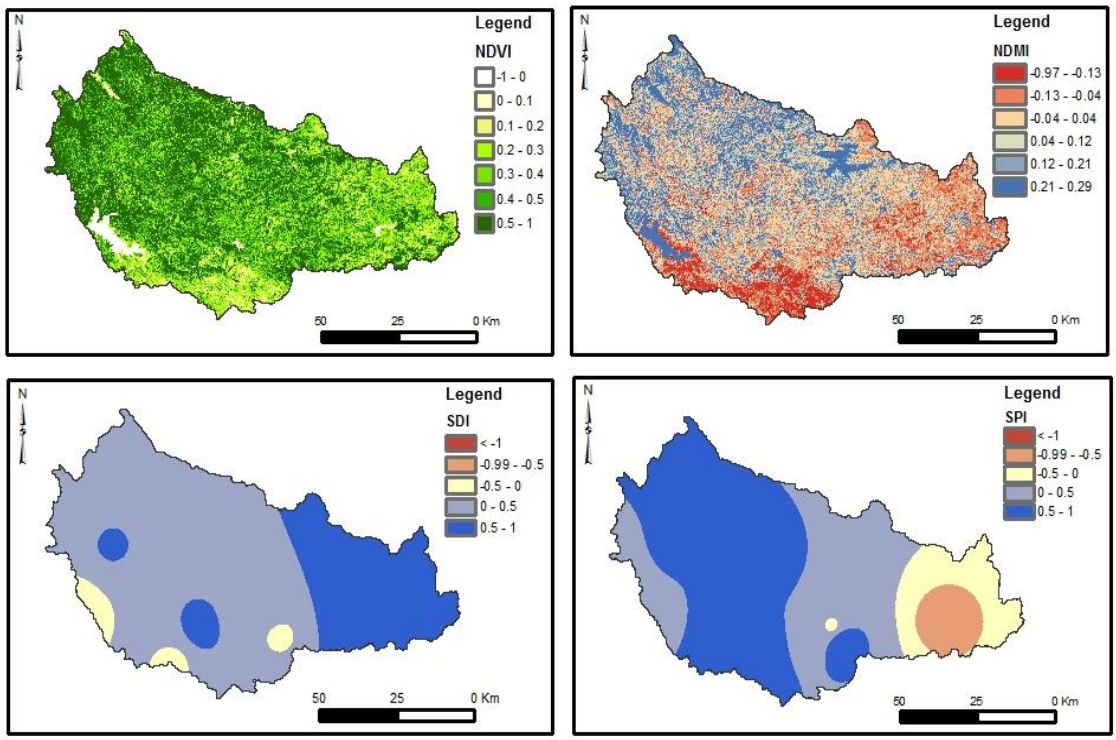

Figure 14. Spatial distribution maps of environmental variables and drought indices in the Ouergha catchment in 2016.

The SPI spatial distribution in Figure 13 indicated mild drought in the 51% of the eastern part of the catchment. Additionally, hydrological drought affected 51% of the area affected by moderate drought in the lower and eastern parts of the catchment. However, meteorological and hydrological drought did not affect vegetation cover (93%) or humidity levels (moisture level = 68%). This could be attributed to the presence of dams that provide irrigation in the area. These dams played a role in maintaining the vegetation cover and humidity levels during the dry event of 2007 and contribute to the preservation of the density and moisture vegetation in the catchment.

The meteorological dry event of 2016 (Figure 14) was mild in the southeastern part of the catchment, and hydrological drought was mild in the eastern part of the catchment. Compared to the last dry event (2007), the vegetation cover and humidity decreased slightly, especially in the lower part of the catchment, with moisture level and vegetation cover values of 90% and 62%, respectively.

4. Discussion

In this study, we aimed to investigate the relationship between climate oscillations, precipitation and flow variability, by comparing the NAO and WeMOi indices of climate fluctuations in the Ouergha catchment with the SPI and SDI from 1984/85 to 2016/17. Our results show that the Ouergha Catchment was exposed to varying intensities of moderate to severe meteorological and hydrological droughts in 1992/93, 1994/95, 1998/99, 2004/05, 2006/07, and 2015/16. The drought analysis showed that during these dry events, the precipitation and flow rate were below the average values of 400 mm and 100 m3/s, respectively. The SPI values show that the highest value of drought for the total period study was -1.32 in 1998/99. The SDI registered the highest drought value of -1.81 in 1994/95.

The temporal variations are dominant by the atmospheric oscillations influence. The positive phase of NAOi (NAOi+) is manifested by lower precipitations, conversely to the negative phase (NAOi-) that expresses climatic disturbances in favor of rainy periods [40]. Moreover, the WeMOi positive phase (WeMoi+) is expressed by precipitations shortage and important precipitations during the negative phase (WeMoi-). The resulting correlations between SPI and NAOi as well as between SPI and WeMOi have a large negative correlation. The general consensus approves that the NAOi has a major influence on climate variability in Morocco [6,10,41,42]. As for the influence of WeMoi on precipitation, Zamrane [18] shows in her study, that WeMoi has an influence on climatic variability but not as important as NAOi.

In our study, both NAOi and WeMoi influence the climatic variability on Ouergha catchment, but the WeMoi is better correlated than the NAOi with the SPI of Ouergha, from October to March with a larger negative correlation of $|r| < -0.60$, except for July and August. However, the large negative correlation between SPI and WeMoi may explain the strong influence. This is perhaps because drought is primarily associated with WeMOi patterns. The correlation between the meteorological (SPI) and hydrological (SDI) drought indices indicated a strong linear link. Thus, meteorological and hydrological droughts emerge in the same year. This result agrees with previous studies in different areas [15,26,43]. Unlike Nalbantis and Tsakiris [22] study that showed a delay of one month (lag 1) between the SPI and SDI drought indices. Indeed, we acknowledge that hydrological drought could be related to many factors such as physical characterization of the catchment, geology, soil occupation and land use/ cover [26]. Therefore, it is imperative to conduct additional research to elucidate the underlying drivers behind the correlation among vegetation

cover, agricultural practices, and their influence on dam functionality. This will enable the development of robust adaptation strategies to mitigate the impact of climate change. Moreover, with climate change accelerating, it is highly likely that the existing dams may prove insufficient to meet the increasing water demands of the region. For instance, changes in precipitation patterns and temperature may result in reduced water availability and increased evapotranspiration rates, which could negatively impact on both the stored and useful volume of water in the dam. Although we acknowledge the importance of other factors, such as physical characterization of the basin, geology, and land use/cover, it is critical to consider the potential impact of climate change on dam usefulness. The response of the hydrometeorological stations to drought was investigated using the Mann–Kendall test (at a significance level of 0.05) during the study period. The results showed a negative trend during dry events, with varying degrees of intensity across the stations. The meteorological stations in the catchment (except for Asfalou, Bab Ouender, and Jbel Outka) received less rain during rainy months stations. All stations except Bab Ouender will likely be exposed to hydrological drought in the future. Moreover, meteorological and hydrological drought helped highlight the impact on vegetation and agricultural development in the Ouergha catchment.

The spatial distribution of drought indices during dry events demonstrates a great influence on vegetation cover and moisture (NDVI and NDMI) in the catchment. During the study period, the density of vegetation cover decreased by 27% in 1998/99. Furthermore, spatial analysis of the SPI and SDI showed that drought events primarily affected the eastern and southern parts of the catchment, whereas the western part was less vulnerable to dry events. In the last 10 years, the presence of dams has supported vegetation cover, especially in nearby irrigated areas. In addition, precipitations variability influenced vegetation densification.

However, precipitations and flow regression do not explain the decline in vegetated land cover, which could also be linked to human activities. Vegetation cover is related to agricultural activities in the Ouergha Catchment and is low during dry events. Thus, the dams supply sufficient water during short dry events but not year-long droughts. Therefore, further studies are required in the Ouergha catchment to explore the relationship between vegetation cover, agricultural activities, and their impact on dam operation and to develop effective strategies for climate change adaptation.

5. Conclusions

The aim of this study was to assess the trends and spatial patterns of drought occurrence in the Ouergha catchment in northern Morocco. To do so, we utilized various data sources including the NAOi, WeMOi, SPI, SDI, NDVI, and NDMI from 1984/85 to 2016/17. Our findings reveal that the Ouergha catchment experienced moderate to severe meteorological and hydrological droughts in different years during the study period. These droughts were characterized by low precipitation and flow rates. The NAOi and WeMOi were found to have an important influence on the climatic variability in the Ouergha catchment, with the WeMOi being more strongly correlated with the SPI, especially from October to March. The correlation between meteorological (SPI) and hydrological (SDI) droughts was strong and linear. The Mann–Kendall test results indicate a negative trend during dry events at the hydrometeorological stations, with varying intensity levels. The spatial distribution of drought indices showed that eastern and southern parts of the catchment were more vulnerable to dry events, while the western part was less affected. However, the strong correlation between meteorological and hydrological droughts and their negative impact on vegetation cover demonstrate

the need for effective drought management strategies in the region. Despite the presence of dams, which helped support vegetation cover, the decline in vegetation cover cannot be solely explained by precipitations and flow regression and could be linked to human activities as well, such as agricultural activities in the Ouergha catchment.

Conflict of interest

We confirm that there is no conflict of interest regarding this manuscript.

References

1. IPCC (2021) Climate Change 2021: The Physical Science Basis. Contribution of Working Group I to the Sixth Assessment Report of the Intergovernmental Panel on Climate Change, 82.
2. Vogt JV, Somma F (2013) Drought and Drought Mitigation in Europe. in Advances in Natural and Technological Hazards Research, vol. 14, Kluwer Academic Publishers, 2000. https://doi.org/10.1007/978-94-015-9472-1
3. La Jeunesse I (2016) Changement climatique et cycle de l'eau-Impacts, adaptation, législation et avancées scientifiques. *Vecteur Environ* 49: 70. https://doi.org/10.51257/a-v1-p4242
4. Bressers H, Bressers N, Kuks S, et al. (2016) The governance assessment tool and its use. *Governance for drought resilience: land and water drought management in Europe* 2016: 45–65. https://doi.org/10.1007/978-3-319-29671-5_3
5. Tramblay Y, El Adlouni S, Servat É (2013) Trends and variability in extreme precipitation indices over Maghreb countries. *Nat Hazards and Earth Syst Sci* 13: 3235–3248. https://doi.org/10.5194/nhess-13-3235-2013
6. Driouech F, Rached SB, Hairech TE (2013) Climate variability and change in North African countries. *Climate change and food security in West Asia and North Africa* 2013: 161–172. https://doi.org/10.1007/978-94-007-6751-5_9
7. MDCE, Troisième Communication Nationale du Maroc à la Convention Cadre des Nations Unies sur les Changements Climatiques., Rabat, Maroc: Ministère Délégué auprès du Ministre de l'Energie, des Mines, de l'Eau et de l'Environnement, Chargé de l'Environnement, 2016. Available from: https://unfccc.int/documents/128109.
8. IPCC, The Physical Science Basis. Contribution of Working Group I to the Fifth Assessment Report of the Intergovernmental Panel on Climate Change, 2013. Available from: https://www.ipcc.ch/site/assets/uploads/2017/09/WG1AR5_Frontmatter_FINAL.pdf.
9. Verner D, Treguer D, Redwood J, et al. (2018) Climate variability, drought, and drought management in Morocco's agricultural sector. https://doi.org/10.1596/30604
10. Driouech F, Stafi H, Khouakhi A, et al. (2021) Recent observed country-wide climate trends in Morocco. *Int J Climatol* 41: E855–E874. https://doi.org/10.1002/joc.6734
11. Mera YEZ, Vera JFR, Pérez-Martín MÁ (2018) Linking El Niño Southern Oscillation for early drought detection in tropical climates: The Ecuadorian coast. *Sci Total Environ* 643: 193–207. https://doi.org/10.1016/j.scitotenv.2018.06.160

12. Vazifehkhah S, Kahya E (2019) Hydrological and agricultural droughts assessment in a semi-arid basin: Inspecting the teleconnections of climate indices on a catchment scale. *Agric Water Manag* 217: 413–425. https://doi.org/10.1016/j.agwat.2019.02.034
13. Mohammadrezaei M, Soltani S, Modarres R (2020) Evaluating the effect of ocean-atmospheric indices on drought in Iran. *Theor Appl Climatol* 140: 219–230. https://doi.org/10.1007/s00704-019-03058-6
14. Ndehedehe CE, Agutu NO, Ferreira VG, et al. (2020) Evolutionary drought patterns over the Sahel and their teleconnections with low frequency climate oscillations. *Atmos Res* 233: 104700. https://doi.org/10.1016/j.atmosres.2019.104700
15. Wei J, Wang WG, Huang Y, et al. (2021) Drought variability and its connection with large-scale atmospheric circulations in Haihe River Basin. *Water Sci Eng* 14: 1–16. https://doi.org/10.1016/j.wse.2020.12.007
16. Luppichini M, Barsanti M, Giannecchini R, et al. (2021) Statistical relationships between large-scale circulation patterns and local-scale effects: NAO and rainfall regime in a key area of the Mediterranean basin. *Atmos Res* 248: 105270. https://doi.org/10.1016/j.atmosres.2020.105270
17. Lopez-Bustins JA, Lemus-Canovas M (2020) The influence of the Western Mediterranean Oscillation upon the spatio-temporal variability of precipitation over Catalonia (northeastern of the Iberian Peninsula). *Atmos Res* 236: 104819. https://doi.org/10.1016/j.atmosres.2019.104819
18. Zamrane Z (2016) *Recherche d'indices de variabilité climatique dans des séries hydroclmatiques au Maroc: identification, positionnement temporel, tendances et liens avec les fluctuations climatiques: cas des grands bassins de la Moulouya, du Sebou et du Tensift* (Doctoral dissertation, Université Montpellier; Université Cadi Ayyad (Marrakech, Maroc). Faculté des sciences Semlalia).
19. Hayes MJ, Alvord C, Lowrey J (2007) Drought indices. *Intermountain West Climate Summary* 3: 2–6. https://doi.org/10.1002/0471743984.vse8593
20. McKee TB, Doesken NJ, Kleist J (1993) The relationship of drought frequency and duration to time scales. *In Proceedings of the 8th Conference on Applied Climatology* 17: 179–183
21. Bhuiyan C (2004) Various drought indices for monitoring drought condition in Aravalli terrain of India. *In Proceedings of the XXth ISPRS Congress, Istanbul, Turkey* 2004: 12–23.
22. Nalbantis I, Tsakiris G (2009) Assessment of hydrological drought revisited. *Water Resour Manag* 23: 881–897. https://doi.org/10.1007/s11269-008-9305-1
23. Rouse JW, Haas RH, Schell JA, et al. (1974) Monitoring vegetation systems in the Great Plains with ERTS. *NASA Spec Publ* 351: 309.
24. Kingston DG, Stagge JH, Tallaksen LM, et al. (2015) European-scale drought: understanding connections between atmospheric circulation and meteorological drought indices. *J Climate* 28: 505–516. https://doi.org/10.1175/JCLI-D-14-00001.1
25. Ezzine H, Bouziane A, Ouazar D (2014) Seasonal comparisons of meteorological and agricultural drought indices in Morocco using open short time-series data. *Int J Appl Earth Obs Geoinf* 26: 36–48. https://doi.org/10.1016/j.jag.2013.05.005
26. Boudad B, Sahbi H, Mansouri I (2018) Analysis of meteorological and hydrological drought based in SPI and SDI index in the Inaouen Basin (Northern Morocco). *J Mater Environ Sci* 9: 219–227. https://doi.org/10.26872/jmes.2018.9.1.25

27. Hadri A, Saidi MEM, Boudhar A (2021) Multiscale drought monitoring and comparison using remote sensing in a Mediterranean arid region: a case study from west-central Morocco. *Arab J Geosci* 14: 1–18. https://doi.org/10.1007/s12517-021-06493-w
28. Senoussi S, Agoumi A, Yacoubi M, et al. (1999) Changements climatiques et ressources en eau Bassin versant de I'Ouergha (Maroc). *Hydroécologie Appliquée* 11: 163–182. https://doi.org/10.1051/hydro:1999007
29. Mesrar, H (2016) Modélisation, quantification et définition des facteurs qui contrôlent le risque de l'érosion hydrique. Cas du bassin versant de l'oued Sahla, Rif central, Maroc. https://doi.org/10.1127/zfg/2015/0169
30. Brunet-Moret Y, Roche M (1955) Etude hydrologique de l'Oued Ouergha à M'Jara. *Journées de l'hydraulique* 1955: 117–122.
31. Renard, B (2009) Détection d'évolutions dans les régimes hydrologiques du bassin du Sebou (Maroc).
32. Martin-Vide J, Lopez-Bustins JA (2006) The western Mediterranean oscillation and rainfall in the Iberian Peninsula. International Journal of Climatology: *A J Royal Meteorol Soc* 26: 1455–1475. https://doi.org/10.1002/joc.1388
33. Tucker CJ, Pinzon JE, Brown ME, et al. (2005) An extended AVHRR 8-km NDVI dataset compatible with MODIS and SPOT vegetation NDVI data. *Int J remote Sens* 26: 4485–4498. https://doi.org/10.1080/01431160500168686
34. Hunt Jr ER, Rock BN (1989) Detection of changes in leaf water content using near-and middle-infrared reflectances. *Remote Sens Environ* 30: 43–54. https://doi.org/10.1016/0034-4257(89)90046-1
35. Kendall SB (1975) Enhancement of conditioned reinforcement by uncertainty 1. *J Exp Anal Behav* 24: 311–314. https://doi.org/10.1901/jeab.1975.24-311
36. Gilbert RO (1987) Statistical methods for environmental pollution monitoring. John Wiley & Sons, 336.
37. Modarres R, da Silva VDPR (2007) Rainfall trends in arid and semi-arid regions of Iran. *J Arid Environ* 70: 344–355. https://doi.org/10.1016/j.jaridenv.2006.12.024
38. Cohen J (1988) Statistical power analysis for the behavioral sciences (2nd edition), lawrence erlbaum associates publishers.
39. Antonie ML, Zaïane OR (2004) Mining positive and negative association rules: An approach for confined rules. *In Knowledge Discovery in Databases: PKDD 2004: 8th European Conference on Principles and Practice of Knowledge Discovery in Databases.* Springer Berlin Heidelberg, Pisa, Italy, 27–38. https://doi.org/10.1007/978-3-540-30116-5_6
40. Ilmen R, Benjelloun H, Ouahmane L, et al. (2016) Preliminary study of winter North Atlantic Oscillation on Atlas cedar tree rings in Morocco. Bulletin de l'Institut Scientifique: *Section Sciences de la Vie* 38: 43–50.
41. Knippertz P, Christoph M, Speth P (2003) Long-term precipitation variability in Morocco and the link to the large-scale circulation in recent and future climates. *Meteorol Atmo Phys* 83: 67–88. https://doi.org/10.1007/s00703-002-0561-y
42. Marchane A, Jarlan L, Boudhar A, et al. (2016) Linkages between snow cover, temperature and rainfall and the North Atlantic Oscillation over Morocco. *Clim Res* 69: 229–238. https://doi.org/10.3354/cr01409

43. Akbari H, Rakhshandehroo G, Sharifloo AH, et al. (2015) Drought analysis based on standardized precipitation index (SPI) and streamflow drought index (SDI) in Chenar Rahdar river basin, Southern Iran. *In American Society of Civil Engineers* 2015: 11–22. https://doi.org/10.1061/9780784479322.002

AIMS Press